

Synthesis, effect of γ -ray and electrical conductivity of uranium doped nano LiMn_2O_4 spinels for applications as positive electrodes in Li-ion rechargeable batteries

FOUAD G. EL-METWALY^{1,3}, MORSI M. ABOU-SEKKINA¹, FAWAZ A. SAAD²,
ABDALLA M. KHEDR^{1,2*}

¹Chemistry Department, Faculty of Science, Tanta University, Tanta, Egypt

²Chemistry Department, College of Applied Sciences, Umm Al-Qura University, Makkah, Saudi Arabia

³Chemistry Department, Faculty of Science, Jazan University, Jazan, Saudi Arabia

LiMn_2O_4 is an attractive candidate cathode material for Li-ion rechargeable batteries, but it suffers from severe capacity fading, especially at higher temperature (55 °C) during charging/discharging processes. Recently, many attempts have been made to synthesize modified LiMn_2O_4 . In this work, a new study on the synthesis of pure and U^{4+} -doped nano lithium manganese oxide [$\text{LiMn}_{2-x}\text{U}_x\text{O}_4$, ($x = 0.00, 0.01, 0.03$)] via solid-state method was introduced. The synthesized $\text{LiMn}_{1.97}\text{U}_{0.03}\text{O}_4$ was irradiated by γ -radiation (10 and 30 kGy). The green samples and the resulting spinel products were characterized using thermogravimetric and differential thermal analysis (TG/DTA), X-ray diffraction (XRD), infrared (IR), and scanning electron microscopy (SEM) measurements. XRD and SEM studies revealed nano-sized particles in all prepared samples. Direct-current (DC) electrical conductivity measurements indicated that these samples are semiconductors and the activation energies decrease with increasing rare-earth U^{4+} content and γ -irradiation. ΔE_a equals to 0.304 eV for $\text{LiMn}_{1.99}\text{U}_{0.01}\text{O}_4$, ΔE_a is 0.282 eV for $\text{LiMn}_{1.97}\text{U}_{0.03}\text{O}_4$ and decreases to $\Delta E_a = 0.262$ eV for γ -irradiated $\text{LiMn}_{1.97}\text{U}_{0.03}\text{O}_4$ nano spinel. The data obtained for the investigated samples increase their attractiveness in modern electronic technology.

Keywords: U^{4+} -doped nano lithium manganates; γ -ray effect; electrical conductivity

© Wrocław University of Technology.

1. Introduction

Since three decades lithium-ion batteries (LIBs) have been the most promising chemical-electrical energy converters (rechargeable or secondary sources) for power electronic devices, such as portable electric devices, cameras, laptops, cellular phones, and many power suppliers. The LIBs based on carbon, a non-aqueous electrolyte, and lithium cobaltate (LiCoO_2) will offer the first rechargeable battery technology for personal electronics in the near future [1, 2]. Now, this technology is applied in green transportation systems, such as electric vehicles (EVs) or hybrid EVs (HEVs). The increase in the demand of highly

functionalized applications always includes higher energy density, higher power density, more safety, and excellent charge-discharge cycling performance.

The element that limits the performance of the batteries is the active element of the positive electrode, and it is the most expensive part. Since more than three decades sustained efforts have been devoted by Goodenough to propose and study oxide compounds based on transition-metal (TM) elements with a special focus to those compounds that crystallize in structures favoring large mobility of Li^+ ions in order to transfer energy during the redox reaction. Milestones were made in 1980 for the LiCoO_2 layered structure [3], for LiMn_2O_4 spinels [4, 5] and for the LiMPO_4 ($M = \text{Fe}, \text{Mn}, \text{etc.}$) olivine family [6]. All these

*E-mail: abkhedr2010@yahoo.com

materials have been studied and applied to the construction of commercial Li-ion batteries. Layered materials are used as cathodes for high-energy systems [7, 8], while spinel oxides and olivines are used in high-power Li-ion batteries because of low cost and long-life requirements, respectively [9, 10]. These lithium-insertion compounds must have specific properties, such as chemical stability, rate capability, capacity, toxicity, safety, and low cost.

In recent years several attempts have been made for synthesizing modified LiMn_2O_4 doped with various elements to inhibit capacity fading and improve the electrochemical performance. For instance the nonmetals B [11], S [12], F [13], Br [14], and the metals Mg [15], Al [16], Ti [17], V, Cr [18], Co [19], Ni [20], Cu [21], Zn [22], Ga [23], Zr [24], Ru [25], Ag [26, 27], Sn [28], Au [29], were used. The substitution increases the average oxidation state of Mn above 3.5, and hence, suppressing Jahn-Teller distortion, stabilizes the crystal structure of the spinel. All dopant elements are less or close to that of Mn, but few reports about the rare-earth elements have been published [30–35]. Here, we aim to go further and use uranium for metal substitution of LiMn_2O_4 spinel. Uranium was chosen as the most common element of actinides and because it is a symbolic element being the last natural element in the periodic table. In this study, only small amounts of dopant has been required, since this is sufficient to strengthen the spinal stability due to stronger M–O bonds of heavy transition metals.

2. Experimental

2.1. Samples preparation

Pure and U^{4+} -doped nano lithium manganese oxide $\text{LiMn}_{2-x}\text{U}_x\text{O}_4$, ($x = 0.00, 0.01, 0.03$) spinels were synthesized via a conventional solid-state procedure. Stoichiometric amounts of the reactants; $\text{LiOH}\cdot\text{H}_2\text{O}$ (99 %) and manganese carbonate (99.5 %) were carefully mixed and appropriate amounts of uranium nitrate (Merck) were added. The mixtures were milled to assure a uniform distribution of the small amounts of dopants. Then,

the mixtures were pre-sintered at 600 °C for 4 h. Finally, the samples were reground and pressed into pellets and sintered in air at 850 °C for 8 h, with a heating rate of 10 °C/min. After sintering, the furnace was slowly cooled to room temperature.

2.2. Instruments used

Thermal gravimetric analysis (TGA) of green (uncalcined) samples was carried out in a dynamic nitrogen atmosphere ($20 \text{ mL}\cdot\text{min}^{-1}$) with a heating rate of $10 \text{ }^\circ\text{C}\cdot\text{min}^{-1}$ using a Shimadzu TG-50 thermo-gravimetric analyzer. Differential thermal analysis was carried out by a Du Pont Instruments 990 thermal analyzer (UK) with a heating rate of $10 \text{ }^\circ\text{C}\cdot\text{min}^{-1}$. The crystal structure of the synthesized spinels was identified by a Philips X-ray diffractometer (PW 1729 X-ray generator, PW 1840 diffractometer control, PM 8203A one line recorder) using $\text{CuK}\alpha$ radiation ($k = 1.54056 \text{ \AA}$) operating at 40.0 kV/30.0 mA. The data were collected in the 2θ range from 10° to 80° . IR spectra of KBr pallets were recorded using a PerkinElmer 1430 IR spectrophotometer within 1000 to 200 cm^{-1} range at the Central Laboratory, Tanta University. The morphology of the products was investigated by scanning electron microscopy (SEM, JSM-5300LV, Japan). DC electrical conductivity of all samples sintered at 850 °C for 8 h was measured using a two-terminal DC electrical conductivity method. The pellets of the samples were coated with silver paste and inserted between the two copper probes of the circuit using an AKeithly 175 multimeter (USA). This was done in the temperature range from room temperature up to 370 °C.

2.3. Effect of γ -ray

$\text{LiMn}_{1.97}\text{U}_{0.03}\text{O}_4$ spinel was exposed to different doses of γ -radiation at National Center for Radiation Research and Technology, Nasr City, Cairo, Egypt. An Indian ^{60}Co gamma cell (2000 Ci) was used as a gamma ray source with a dose rate of 1.5 Gy/sec (150 rad/sec) [36]. Gy (gray) is the SI unit of absorbed dose and it is expressed as $\text{m}^2\cdot\text{s}^{-2}$ [37].

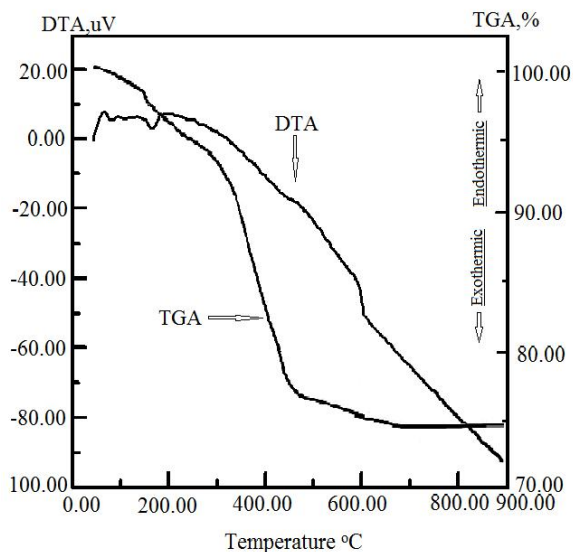


Fig. 1. TGA/DTA curves of the precursor fired to form LiMn_2O_4 doped nano spinel.

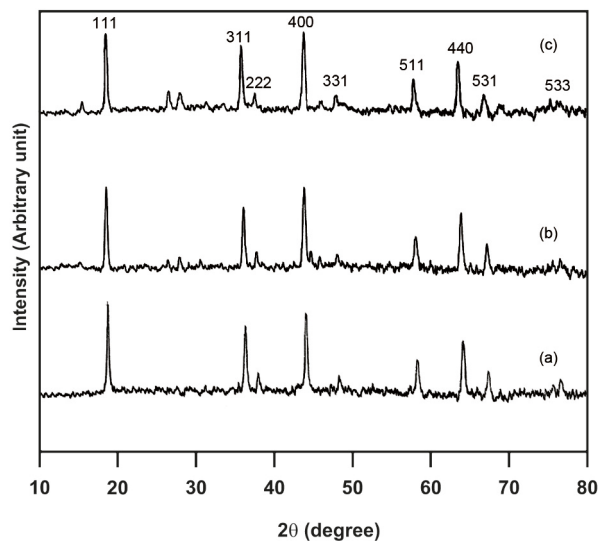


Fig. 2. X-ray diffraction patterns of $\text{LiMn}_{2-x}\text{U}_x\text{O}_4$: (a) undoped LiMn_2O_4 , (b) $\text{LiMn}_{1.99}\text{U}_{0.01}\text{O}_4$, (c) $\text{LiMn}_{1.97}\text{U}_{0.03}\text{O}_4$.

3. Results and discussion

3.1. Thermal studies

TGA/DTA curves of the precursor that was fired to give U-doped LiMn_2O_4 nano spinels are presented in Fig. 1. The obtained results indicate that weight losses occur mainly in three steps. In the first step, a weight loss occurs in the temperature range of 80 to 110 °C gradually, due to evaporation of moisture corresponding to weak peak at 82 °C in the DTA curve. In the second step, the weight loss occurring within 180 to 300 °C temperature range, as a result of decomposition LiOH to Li_2O and volatilization of H, corresponds to the weak peak at 180 °C in the DTA curve. In the third step, the weight loss within 310 to 680 °C temperature range is due to the combustion of organic constituents followed by successive phase transfer steps to reach the most stable spinel phase at 900 °C.

3.2. X-ray diffraction studies

The Cu $K\alpha$ powder X-ray diffraction (XRD) patterns of the synthesized pure and doped spinels ($\text{LiMn}_{2-x}\text{U}_x\text{O}_4$) with different content of U^{4+} ($x = 0.00, 0.01, 0.03$) are presented in Fig. 2. All diffraction peaks are very strong, which indicates that all samples have a good cubic crystal structure

corresponding to cubic standard LiMn_2O_4 structure with the space group $\text{Fd}3\text{m}$ [38]. It includes a cubic close-packing arrangement of oxygen ions at the 32 e sites. The Li ions are at the tetrahedral 8a sites, and the Mn^{3+} and Mn^{4+} ions are at the octahedral 16 d sites [39]. The lattice constant and crystal volume of U^{4+} doped spinels are bigger than that of the pure one and they are increasing with increasing the doping content (Table 1). The radius of U^{4+} (0.89 Å) is bigger than the radius of Mn^{3+} (0.66 Å). This confirms that U^{4+} locates at the position of Mn^{3+} in MnO_6 octahedral sites. Fig. 3 shows X-ray diffraction patterns of $\text{LiMn}_{1.97}\text{U}_{0.03}\text{O}_4$ spinel γ -irradiated with 10 kGy and 30 kGy. All diffraction peaks are very strong, which indicates that the samples have a good cubic crystal structure but with the peaks shifted to lower angles. Gamma rays are an ionizing radiation and refer to electromagnetic radiation of extremely high frequency and therefore high energy per photon. Gamma radiation is produced by the decay from high energy states of atomic nuclei (gamma decay) and other processes.

Ultra-high energy gamma-ray refers to gamma radiation with short wavelengths (between 10^{-20} and 10^{-23} meter), and photon energies

Table 1. Unit cell parameters and crystallite size of LiMn_2O_4 , non irradiated and γ -irradiated $\text{LiMn}_{2-2x}\text{U}_x\text{O}_4$ nano spinels.

No.	Sample	Lattice constant a (Å)	Unit cell volume (Å ³)	Crystallite size × 10 ⁹ nm
1.	LiMn_2O_4	8.17	545.34	15.31
2.	$\text{LiMn}_{1.99}\text{U}_{0.01}\text{O}_4$	8.24	559.48	15.32
3.	$\text{LiMn}_{1.97}\text{U}_{0.03}\text{O}_4$	8.27	565.61	16.58
4.	$\text{LiMn}_{1.97}\text{U}_{0.03}\text{O}_4$ γ -irradiated with 10 kGy	8.33	578.01	17.69
5.	$\text{LiMn}_{1.97}\text{U}_{0.03}\text{O}_4$ γ -irradiated with 30 kGy	8.34	580.09	18.97

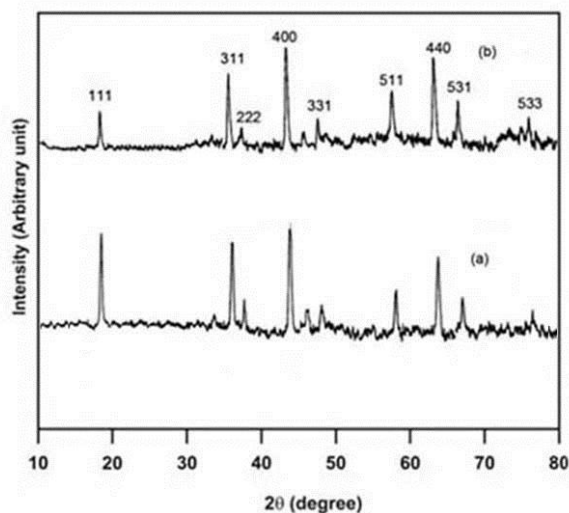


Fig. 3. X-ray diffraction patterns of γ -irradiated $\text{LiMn}_{1.97}\text{U}_{0.03}\text{O}_4$: (a) $\text{LiMn}_{1.97}\text{U}_{0.03}\text{O}_4$ spinel γ -irradiated with 10 kGy, (b) $\text{LiMn}_{1.97}\text{U}_{0.03}\text{O}_4$ spinel γ -irradiated with 30 kGy.

within 10^{14} to 10^{17} electron-volts (eV) range [40]. When a gamma ray passes through matter, the probability for absorption is proportional to the thickness of the layer, the density of the material, and the absorption cross section of the material. High energy gamma rays (exceeding 10 MeV) have the ability to interact with atomic nuclei, which results in ejection of particles in photodisintegration or, in some cases, even nuclear fission (photofission) [41]. The lattice constant and crystal volume of γ -irradiated samples are slightly bigger than those of non γ -irradiated ones (Table 1) indicating high stability of the doped samples against this type of great energy (γ -rays).

3.3. IR spectral studies

The local environment of the cations in a lattice of close-packed oxygen can be studied by IR spectroscopy. The vibrational modes attributed to the motion of cations with respect to their oxygen neighbors are sensitive to the point group symmetry of the cations in the oxygen host matrix [42, 43]. The room temperature IR spectra of pure and U^{4+} -doped nano LiMn_2O_4 spinels, which were prepared by solid-state method and sintered at 850°C for 8 h are depicted in Fig. 4. The strong bands at 221, 260, 518 and 617 cm^{-1} are assigned to vibration modes of MnO_6 octahedron. The band at 260 cm^{-1} is attributable to mixed character of octahedral MnO_6 and tetrahedral LiO_4 , building the cubic lattice of nano LiMn_2O_4 . The obtained infrared spectra of the lattice vibration show broad and interfering peaks, where the structure of LiMn_2O_4 exhibits a charge disproportion, such as $\text{LiMn}^{3+}\text{Mn}^{4+}\text{O}_4$. There are isotropic Mn^{4+}O_6 octahedron and locally distorted Mn^{3+}O_6 octahedron due to the Jahn-Teller effect. Stretching vibration of Mn^{4+}O_6 and Mn^{3+}O_6 octahedra provides a shoulder broad peak at about 518 cm^{-1} and strong broad peak at 617 cm^{-1} of the $\nu_{as}(\text{Mn-O})$ mode. The IR bands at 221 and 260 cm^{-1} have mixed character due to the presence of the bending modes of O–Mn–O bands and modes of LiO_4 group leading to the interference between the peaks. This is a characteristic spectrum of LiMn_2O_4 spinel [44, 45]. Also, the IR spectra of U^{4+} doped spinel consist of overlapped peaks characteristic of Li–Mn–O spinel. For nano $\text{LiMn}_{1.99}\text{U}_{0.01}\text{O}_4$, the main bands at 221, 518, and 617 cm^{-1} are shifted to 224, 519, and 614 cm^{-1} . For $\text{LiMn}_{1.97}\text{U}_{0.03}\text{O}_4$,

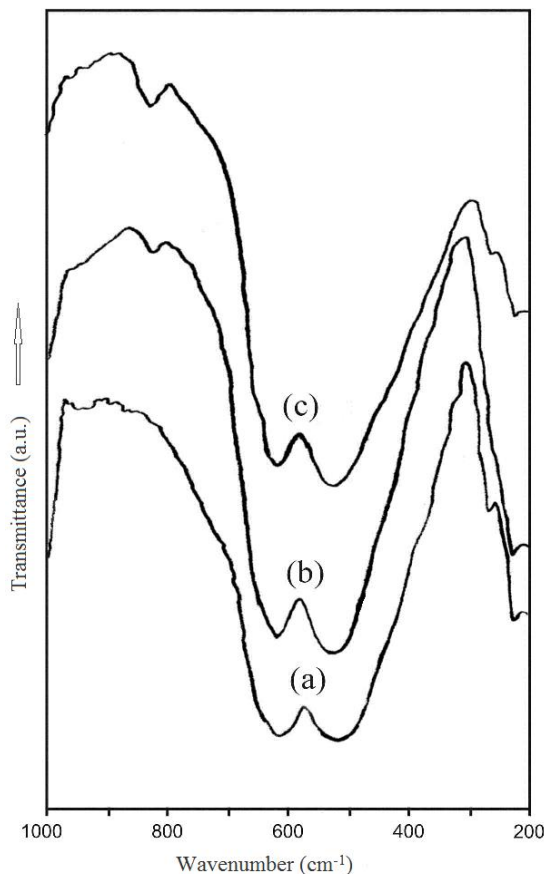


Fig. 4. IR absorption spectra of $\text{LiMn}_{2-x}\text{U}_x\text{O}_4$ fired at 850°C in air for 8 h: (a) undoped LiMn_2O_4 spinel, (b) doped $\text{LiMn}_{1.99}\text{U}_{0.01}\text{O}_4$ spinel, (c) doped $\text{LiMn}_{1.97}\text{U}_{0.03}\text{O}_4$ spinel.

the peaks at 221 , 518 and 617 cm^{-1} are shifted to 220 , 519 and 613 cm^{-1} , respectively. This is a good evidence for the partial substitution of Mn^{3+} with U^{4+} in the octahedral site. Fig. 5 represents the IR spectra of $\text{LiMn}_{1.97}\text{U}_{0.03}\text{O}_4$ samples γ -irradiated with 10 and 30 kGy. There are very slight changes in crystal vibration modes in case of γ -irradiated samples compared with non-irradiated ones, which indicates high stability of the spinels against γ -irradiation. All IR spectral data confirm the data obtained from X-ray diffraction studies.

3.4. SEM investigation

The morphology of pure and doped samples was investigated by scanning electron microscopy (SEM) after coating the samples with gold. Fig. 6 shows SEM images of

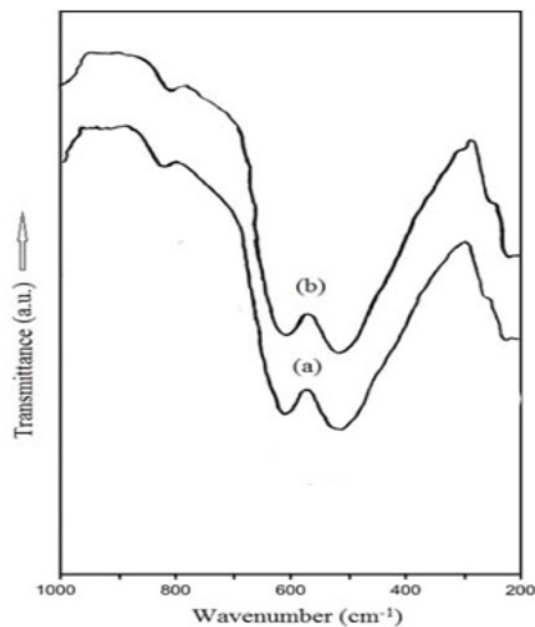


Fig. 5. IR absorption spectra of γ -irradiated $\text{LiMn}_{1.97}\text{U}_{0.03}\text{O}_4$: (a) $\text{LiMn}_{1.97}\text{U}_{0.03}\text{O}_4$ spinel γ -irradiated with 10 kGy, (b) $\text{LiMn}_{1.97}\text{U}_{0.03}\text{O}_4$ spinel γ -irradiated with 30 kGy.

LiMn_2O_4 , $\text{LiMn}_{1.99}\text{U}_{0.01}\text{O}_4$, $\text{LiMn}_{1.97}\text{U}_{0.03}\text{O}_4$, and γ -irradiated (30 kGy) $\text{LiMn}_{1.97}\text{U}_{0.03}\text{O}_4$ spinels. The images show irregular porous morphology, which is beneficial for the diffusion of electrolyte into the interior of the particle during fabrication of the spinel, and reveal that the powder exhibits nano particles size. It consists of nano single crystals with the size in the range of 15 to 19 nm depending on the values of crystal size calculated from X-ray patterns using Scherer's equation [46] (Table 1).

3.5. DC-electrical conductivity studies

Fig. 7 shows the measured DC electrical conductivity ($\ln\sigma$) of doped samples before and after irradiation as a function of the reciprocal of absolute temperature. We have used Arrhenius equation: $\sigma = \sigma^\circ e^{-\Delta E_a/k_B T}$, where σ is the electrical conductivity at absolute temperature T , k_B is Boltzmann's constant = $8.61 \times 10^{-5}\text{ eV}\cdot\text{K}^{-1}$, σ° is the maximum electrical conductivity (that it would have at infinite temperature), and ΔE_a is the activation energy for electrical conduction, which indicates the energy needed for an ion to jump to a free

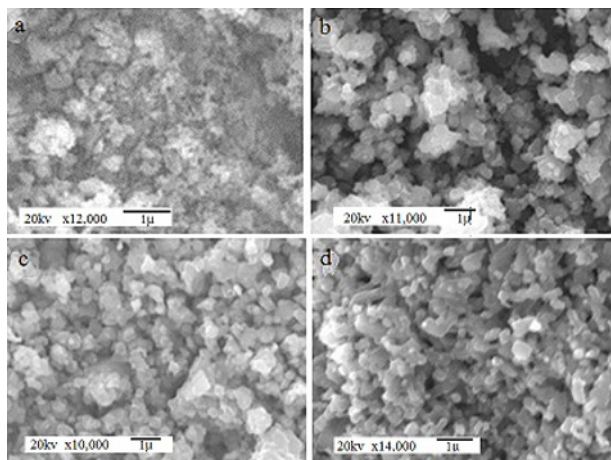


Fig. 6. SEM images of LiMn_2O_4 spinel (a), $\text{LiMn}_{1.99}\text{U}_{0.01}\text{O}_4$ spinel (b), $\text{LiMn}_{1.97}\text{U}_{0.03}\text{O}_4$ spinel (c), and $\text{LiMn}_{1.97}\text{U}_{0.03}\text{O}_4$ spinel irradiated with 30 kGy (d).

hole [47]. The conductivity increases with increasing temperature, which indicates semi-conducting behavior for both non-irradiated and γ -irradiated samples. The conduction in LiMn_2O_4 nano spinel is based on small-polaron hopping between Mn^{3+} and Mn^{4+} , i.e. unpaired electrons from e_g orbitals of high spin Mn^{3+} (d_4) hop to neighboring low-spin Mn^{4+} (d_3) ions. Both the e_g orbitals of metal ion are equivalent in energy because they lie on the same octahedral site [48]. The samples display extrinsic semiconducting behavior in a wide temperature range with activation energy (ΔE_a) equal to 0.304 eV for $\text{LiMn}_{1.99}\text{U}_{0.01}\text{O}_4$. The activation energy reduces for $\text{LiMn}_{1.97}\text{U}_{0.03}\text{O}_4$ to 0.282 eV with increasing dopant content. ΔE_a equals to 0.262 eV for γ -irradiated (30 kGy) $\text{LiMn}_{1.97}\text{U}_{0.03}\text{O}_4$ nano spinel. In conclusion, the activation energies of conduction of the prepared U^{4+} doped nano samples reduce with increasing dopant content and γ -irradiation.

4. Conclusions

Pure nano LiMn_2O_4 , non-irradiated and γ -irradiated rare-earth U^{4+} -doped lithium manganate spinels [$\text{LiMn}_{2-x}\text{U}_x\text{O}_4$] were synthesized using a simple solid-state method. X-ray diffraction data revealed the formation of single-phase spinel

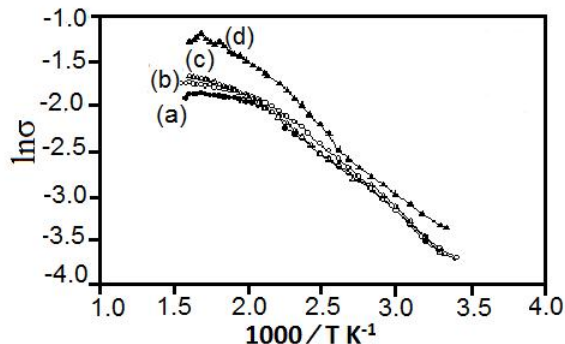


Fig. 7. Variation of DC electrical conductivity ($\ln\sigma$) versus reciprocal of absolute temperature [$(1000/T) \text{ K}^{-1}$] for non irradiated $\text{LiMn}_{1.99}\text{U}_{0.01}\text{O}_4$ (a), non irradiated $\text{LiMn}_{1.97}\text{U}_{0.03}\text{O}_4$ (b), $\text{LiMn}_{1.97}\text{U}_{0.03}\text{O}_4$ spinel γ -irradiated with 10 kGy (c), and $\text{LiMn}_{1.97}\text{U}_{0.03}\text{O}_4$ spinel γ -irradiated with 30 kGy (d).

with cubic crystal structure for pure and doped samples. Also, X-ray diffraction calculations and SEM images confirmed that the synthesized spinels are nano compounds of crystal size in the range of 15 to 19 nm with porous morphology. The electrical studies revealed the improvement of electrical properties of the non irradiated and γ -irradiated U^{4+} -doped lithium manganate spinels compared with pure LiMn_2O_4 . The method used for the preparation has a great potential for the commercial preparation of pure LiMn_2O_4 and doped nano $\text{LiMn}_{2-x}\text{U}_x\text{O}_4$ spinels.

References

- [1] JULIEN C.M., MAUGER A., ZAGHIB K., GROULT H., *Inorganics*, 2 (2014), 132.
- [2] NAGaura T., TOZAWA K., *Prog. Batteries Sol. Cells*, 9 (1990), 209.
- [3] MIZUSHIMA K., JONES P.C., WISEMAN P.J., GOODENOUGH J.B., *Mater. Res. Bull.*, 15 (1980), 783.
- [4] THACKERAY M.M., DAVID W.I.F., BRUCE P.G., GOODENOUGH J.B., *Mater. Res. Bull.*, 18 (1983), 461.
- [5] THACKERAY M.M., JOHNSON P.J., DE PICCIOTTO L.A., BRUCE P.G., GOODENOUGH J.B., *Mater. Res. Bull.*, 19 (1984), 179.
- [6] PADHI A.K., NANJUNDASWAMY K.S., GOODENOUGH J.B., *J. Electrochem. Soc.*, 144 (1997), 1188.
- [7] PERES J.P., WEILL F., DELMAS C., *Solid State Ionics*, 116 (1999), 19.
- [8] OHZUKU T., MAKIMURA Y., *Chem. Lett.*, 30 (2001), 642.

- [9] TARASCON J.M., MC KINNON W.R., COOWAR F., BOWMER T.N., AMATUCCI G., GUYOMARD D., *J. Electrochem. Soc.*, 141 (1994), 1421.
- [10] ZAGHIB K., MAUGER A., GROULT H., GOODENOUGH J.B., JULIEN C.M., *Materials*, 6 (2013), 1028.
- [11] CHAN H.W., DUH J.G., SHEEN S.R., *Surf. Coat. Tech.*, 188 (2004), 116.
- [12] MOLENDI M., DZIEMBAJ R., PODSTAWKA E., PRONIEWICZ L.M., PIWOWARSKA Z., *J. Power Sources*, 174 (2007), 613.
- [13] JAVAPRAKASH N., KALAISELVI N., DOH C.H., GAN-GULIBABU, BHUVANESWARI D., *J. Appl. Electrochem.*, 40 (2010), 2193.
- [14] DU G., SHARMA N., PETERSON V.K., KIMPTON J.A., JIA D., GUO Z., *Adv. Funct. Mater.*, 21 (2011), 3990.
- [15] SINGH P., SIL A., NATH M., RAY S., *Ceram.-Silikaty*, 54 (2010), 38.
- [16] AMARAL F.A., BOCCHI N., BROCCENSI R.F., BIGAGGIO S.R., ROCHA-FILHO R.C., *J. Power Sources*, 195 (2010), 3293.
- [17] LIU D.Q., LIU X.Q., HE Z.Z., *Mater. Chem. Phys.*, 105 (2007), 362.
- [18] SAAD F.A., ABOU-SEKKINA M.M., KHEDR A.M., EL-METWALY F.G., *Int. J. Electrochem. Sc.*, 9 (2014), 3904.
- [19] SAKUNTHALA A., REDDY M.V., SELVASEKARAPANDIAN S., CHOWDARI B.V.R., SELVIN P.C., *Electrochim. Acta*, 55 (2010), 4441.
- [20] WU H.M., TU J.P., CHEN X.T., LI Y., ZHAO X.B., CAO G.S., *J. Solid State Electr.*, 11 (2007), 173.
- [21] EIN ELI Y., URIAN R.C., WEN W., MUKERJEE S., *Electrochim. Acta*, 50 (2005), 1931.
- [22] SCLAR H., HAIK O., MENACHEM T., GRINBLAT J., LEIFER N., MEITAV A., LUSKI S., AURBACH D., *J. Electrochem. Soc.*, 159 (2012), A228.
- [23] LIU D.Q., HE Z.Z., LIU X.Q., *J. Alloy. Compd.*, 440 (2007), 69.
- [24] WU H.M., BELHAROUAK I., ABOUIMRANE A., SUN Y.K., AMINE K., *J. Power Sources*, 195 (2010), 2909.
- [25] WANG H.L., TAN T.A., YANG P., LAI M.O., LUI L., *J. Phys. Chem.*, 115 (2011), 6102.
- [26] SON J.T., PARK K.S., KIM H.G., CHUNG H.T., *J. Power Sources*, 126 (2004), 182.
- [27] ZHOU W.J., HE B.L., LI H.L., *Mater. Res. Bul.*, 43 (2008), 2285.
- [28] WANG L., ZHAO J.S., GUO S.H., HE X.M., JIANG C.Y., WAN C.R., *Int. J. Electrochem. Sci.*, 5 (2010), 1113.
- [29] TU J., ZHAO X.B., CAO G.S., TU J.P., ZHU T.J., *Mater. Lett.*, 60 (2006), 3251.
- [30] SUN H.B., CHEN Y.G., XU C.H., ZHU D., HUANG L.H., *J. Solid State Electr.*, 16 (2012), 1247.
- [31] KHEDR A.M., ABOU-SEKKINA M.M., EL-METWALY F.G., *J. Electron. Mater.*, 42 (2013), 1275.
- [32] BALAJI S.R.K., MUTHARASU D., SHANMUGAN S., SUBRAMANIAN N.S., RAMANATHAN K., *Ionics*, 16 (2010), 351.
- [33] HELAN M., BERCHMANS L.J., KUMARI V.S.S., RAVISANKAR R., SHANMUGAM V.M., *Mater. Res. Innov.*, 15 (2010), 130.
- [34] LI C., FAN Y.L., LI S.Z., XIE B., BI L., YANG S.T., *Rare Metals*, 25 (2006), 58.
- [35] ABOU-SEKKINA M.M., KHEDR A.M., EL-METWALY F.G., *Chem. Mater. Res.*, 3 (2013), 15.
- [36] EL-BATAL F.H., ABO-NAF S.M., EZZLDIN F.M., *Indian J. Pure Appl. Phys.*, 43 (2005), 579.
- [37] DROBNY J.G., *Ionizing Radiation and Polymers: Principles, Technology, and Applications*, 1st ed., William Andrew Publishing, Norwich, 2012.
- [38] LIU Q., WANG S., TAN H., YANG Z., ZENG J., *Energies*, 6 (2013), 1718.
- [39] MANDAL S., ROJAS R.M., AMARILLA J.M., CALLE P., KOSOVA N.V., ANUFRIENKO V.F., ROJO J.M., *Chem. Mater.*, 14 (2002), 1598.
- [40] IKHSANOV N.R., *Astrophys. Space Sci.*, 184 (1991), 297.
- [41] L'ANNUNZIATA M.F., *Radioactivity: Introduction and History*, Elsevier, Amsterdam, 2007.
- [42] ROUGIER C.J., NAZRI G.A., JULIEN C., *Mater. Res. Soc. Symp. Proc.*, 453 (1997), 647.
- [43] ROUGIER C.J., NAZRI G.A., JULIEN C., *Ionics*, 3 (1997), 170.
- [44] HE Z.-Q., XIONG L.-Z., WU X.-M., CHEN S., HUANG K.-L., *Trans. Nonferrous Met. Soc. China*, 20 (2010), s257.
- [45] WANG G.G., WANG J.M., MAO W.Q., SHAO H.B., ZHANG J.Q., CA C.N., *J. Solid State Electr.*, 9 (2005), 524.
- [46] PATTERSON A.L., *Phys. Rev.*, 56 (1939), 978.
- [47] BOCKRIS J.O'M., REDDY A.K.N., *Modern Electrochemistry*, Plenum Press, New York, 1998.
- [48] ABOU-SEKKINA M.M., SAAD F.A., EL-METWALY F.G., KHEDR A.M., *Mater. Sci.-Poland*, in press (2014).

Received 2014-06-23

Accepted 2014-08-14